THE JOURNAL OF BIOLOGICAL CHEMISTRY
Vol. 274, No. 32, Issue of August 6, pp. 22275–22282, 1999

Printed in U.S.A.

The *aroC* Gene of *Aspergillus nidulans* Codes for a Monofunctional, Allosterically Regulated Chorismate Mutase*

(Received for publication, March 17, 1999, and in revised form, May 4, 1999)

Sven Krappmann, Kerstin Helmstaedt, Thomas Gerstberger, Sabine Eckert, Bernd Hoffmann, Michael Hoppert, Georg Schnappauf, and Gerhard H. Braus‡

From the Institute of Microbiology & Genetics, Georg-August-University, Grisebachstrasse 8, D-37077 Göttingen, Germany

The cDNA and the chromosomal locus of the *aroC* gene of *Aspergillus nidulans* were cloned and is the first representative of a filamentous fungal gene encoding chorismate mutase (EC 5.4.99.5), the enzyme at the first branch point of aromatic amino acid biosynthesis. The *aroC* gene complements the *Saccharomyces cerevisiae aro7*Δ as well as the *A. nidulans aroC* mutation. The gene consists of three exons interrupted by two short intron sequences. The expressed mRNA is 0.96 kilobases in length and *aroC* expression is not regulated on the transcriptional level under amino acid starvation conditions. *aroC* encodes a monofunctional polypeptide of 268 amino acids. Purification of this 30-kDa enzyme allowed determination of its kinetic parameters (k_{cat} = 82 s^{-1}, n_H = 1.56, $[S]_{0.5}$ = 2.3 mM), varying pH dependence of catalytic activity in different regulatory states, and an acidic pI value of 4.7. Tryptophan acts as heterotropic activator and tyrosine as negative acting, heterotropic feedback-inhibitor with a K_i of 2.8 μM. Immunological data, homology modeling, as well as electron microscopy studies, indicate that this chorismate mutase has a dimeric structure like the *S. cerevisiae* enzyme. Site-directed mutagenesis of a crucial residue in loop220s (Asp^{233}) revealed differences concerning the intramolecular signal transduction for allosteric regulation of enzymatic activity.

Chorismic acid is the last common compound in the biosynthesis of aromatic amino acids. The metabolic branch leading to L-tryptophan is initiated by its conversion to anthranilate catalyzed by the enzyme anthranilate synthase (EC 4.1.3.27), whereas the catalytic reaction to prephenate finally leads to L-phenylalanine and L-tyrosine (1, 2). The latter reaction is the only known Claisen rearrangement in primary metabolism of living organisms and is catalyzed by a unique enzyme, the chorismate mutase (EC 5.4.99.5) (3). Chorismate mutases are found in archaea, bacteria, fungi, and plants (4). Based on primary sequence information and determination of the crystal structure of three natural enzymes, chorismate mutases are classified into two groups: the chorismate mutase of *Bacillus subtilis* represents the AroH class and is characterized by its trimeric pseudo α/β-barrel structure (5, 6). In contrast, polypeptides of the AroQ class are all-helix bundle proteins and are often part of a bifunctional enzyme containing a chorismate mutase domain (7). According to Hilvert and co-workers (8), eukaryotic chorismate mutases, which additionally contain regulatory domains, also fall into the latter class despite of the rare primary amino acid sequence similarity with their prokaryotic counterparts. The enzymatic properties of some eukaryotic chorismate mutases have been studied in detail, but only a limited number of the corresponding genes have been cloned yet (4).

The chorismate mutase of the bakers' yeast *Saccharomyces cerevisiae* is the most prominent member of the AroQ class and has been characterized in extensive studies (9–11). Its allosteric modulation by tyrosine and tryptophan serves as a model in understanding the regulatory properties of a branch point enzyme. Determination of different crystal structures has given insight into the structural basis for the regulatory processes controlling the flux of chorismate into one of the two branches in the biosynthesis of aromatic amino acids (see Ref. 12, and references therein). In addition, molecular dynamics studies have given hints to understand the mechanism of the enzymatic conversion performed by this enzyme (13). The homodimeric yeast enzyme consists of 2 × 12 helices with the catalytically active domain built up by three helices of each subunit. The loop preceding one of these helices has turned out to be crucial for transmitting the signal of T to R state transition. Conversion of one residue in this loop (T226I) results in a constitutively activated enzyme that is unresponsive to its inhibitor tyrosine (14).

To date, no gene coding for a chorismate mutase of a filamentous fungus has been characterized. Here we present the characterization of the chorismate mutase-encoding gene *aroC* of *Aspergillus nidulans*. This filamentous fungus has become a model organism concerning metabolism as well as differentiation in recent decades (15, 16). The *aroC* gene product was overexpressed in yeast using recombinant DNA technology and then purified for kinetic assays and regulatory analysis. The quarternary structure was determined by computer modeling and compared with the yeast enzyme. Additionally, site-directed mutagenesis was applied to investigate the role of a putatively crucial residue (Asp^{233}) in allosteric transition as this amino acid residue corresponds to residue Thr^{226} in the yeast chorismate mutase. We found that the newly characterized chorismate mutase shares structural similarities with its yeast homologue, but that the molecular basis of the mechanism for T-R transition is not conserved.

EXPERIMENTAL PROCEDURES

Materials—Chorismic acid as barium salt was purchased from Sigma. Ethylamino-Sepharose was prepared following the protocol for activation of Sepharose CL-4B (17) and by coupling of the ligand ethylamine-HCl to the activated matrix. Protein solutions were concentrated by using stirred cells (volumes of 180 and 10 ml) with PM-10

* This work was supported by grants from the Deutsche Forschungsgemeinschaft, Fonds der Chemischen Industrie, Volkswagen-Stiftung, and the Niedersächsischen Vorab der Volkswagen-Stiftung, Forschungsstelle für nachwachsende Rohstoffe. The costs of publication of this article were defrayed in part by the payment of page charges. This article must therefore be hereby marked "*advertisement*" in accordance with 18 U.S.C. Section 1734 solely to indicate this fact.

Dedicated to Prof. Dr. William N. Lipscomb on the occasion of his 80th birthday.

‡ To whom correspondence should be addressed. Tel.: 49-0-551-39-3770; Fax: 49-0-551-39-3820; E-mail: gbraus@gwdg.de.

ultrafiltration membranes from Millipore (Eschborn, Germany). The Mini 2D SDS-polyacrylamide gel electrophoresis system and the Bradford protein assay solution for determination of protein concentrations originated from Bio-Rad. Vent polymerase (BIOLABS, Schwalbach, Germany) was used for polymerase chain reactions. All other chemicals were supplied by FLUKA (Neu-Ulm, Germany) or Sigma-Aldrich Chemie GmbH (Steinheim, Germany).

Strains, Media, cDNA Library, Plasmids, Growth Conditions—The *S. cerevisiae* strain RH2185 (*MATa, suc2-Δ9, ura3-52, leu2-3, leu2-112, his4-519, aro7::LEU2, GAL2*) (10) with the genetic background of the laboratory strain X2180-1A (*MATa, gal2, SUC2, mal, CUP1*) was used as recipient for cloning of an *aroC* cDNA out of an inducible expression library. The expression library was constructed after mRNA isolation from *A. nidulans* strain FGSC A234 (*yA2, pabaA1, veA1*) using the Superscript™ cDNA Synthesis Kit from Life Technologies, Inc. (Gaithersburg, MD). cDNAs were ligated as *SalI*/*Not*I fragments in the shuttle vector pRS316-*GAL1* (18) and propagated in *Escherichia coli*. Yeast transformation was carried out as described in Ref. 19. Transformation of *A. nidulans* was carried out according to Punt and van den Hondel (20). For overexpression, a derivative of plasmid p426MET25 (21) was used in the *S. cerevisiae* strain RH2192 (*MAT**a**, pra1-1, prb1-1, prc1-1, cps1-3, ura3Δ5, leu2-3, 112, his⁻, aro7::LEU2*) which is a derivative of the protease-deficient strain c13-ABYS-86 (22). The *A. nidulans* strain G1100 (*aroC1248, riboA1, adG14, yA2*) was described earlier (23) and was obtained from J. Clutterbuck, Glasgow, United Kingdom. MV minimal medium for the cultivation of yeast was described earlier (24) and minimal medium for the cultivation of *A. nidulans* strains was prepared according to Käfer (25).

Site-directed Mutagenesis—A polymerase chain reaction-based method was used for site-directed mutagenesis of *aroC* (26). The polymerase chain reaction-generated fragments were sequenced (27) to confirm the presence of the mutations and to rule out second-site mutations.

RNA Preparation and Analysis—Total RNA was prepared from vegetatively growing *A. nidulans* cultures using the TRIzol™ reagent from Life Technologies, Inc. following the supplier's instructions. Transcript levels were analyzed by Northern hybridization (28) using a Bio-Imaging Analyzer from Fuji Photo Film Co. Ltd. (Tokyo, Japan). Transcript length was determined using the 0.16–1.77-kb[1] RNA ladder from Life Technologies, Inc.

Overexpression and Purification of A. nidulans Chorismate Mutase—Plasmid-carrying yeast strains were grown at 30 °C in 10-liter rotatory fermentors under aeration. Cells were harvested in mid-log phase at an $OD_{546\ nm}$ of 4–6, washed twice with 50 mM potassium phosphate buffer, pH 7.6, and stored in 1 ml of buffer/g wet cells at −20 °C in the presence of protease inhibitors (0.1 mM phenylmethylsulfonyl fluoride (PMSF), 0.2 mM EDTA, and 1 mM DL-dithiothreitol). For purification, 80–110 g of cells were thawed and run three times through a French Pressure Cell (18,000 p.s.i.). Cell debris was sedimented by centrifugation at 30,000 × *g* for 20 min.

The chorismate mutase was purified according to the protocol of Schmidheini *et al.* (14) with the following modifications: in all steps 10 mM potassium phosphate buffer, pH 7.6, was used as solvent, ammonium sulfate precipitation was carried out at 47% saturation, phenylmethylsulfonyl fluoride was added to the equilibration buffer for the ethylamino-Sepharose column, dialysis was used to desalt protein extracts, and a second run on a Mono Q column at pH 5.8 in 10 mM potassium phosphate buffer was performed. Chorismate mutase was detected by SDS-polyacrylamide gel electrophoresis (29) and enzymatic activity assays. Measurements of protein concentrations were performed using the Bradford assay (30).

Enzyme Assays—Chorismate mutase activity was measured as described previously (9) with some modifications. The enzymatic conversion is stopped after 1 min by addition of HCl and the product of the enzymatic reaction, prephenate, is converted to phenylpyruvate through a chemical reaction. Enzymatic activity is measured spectrophotometrically, determining the concentration of phenylpyruvate. Since absorbance of phenylpyruvate is temperature-dependent due to a keto-enol equilibrium, the assay was standardized by keeping the enzymatic reactions at 30 °C and equilibrating the spectrophotometer cell to the same temperature. Reaction volumes of 250 μl containing 100 mM potassium phosphate, pH 7.6, 2 mM EDTA, 20 mM dithiothreitol, optionally 50 μM tyrosine or 5 μM tryptophan, chorismate mutase enzyme, and chorismate in a range from 0.25 to 13 mM were used. The reaction was started by adding the mixture of all ingredients to the prewarmed chorismate solution. The reaction was stopped by adding 250 μl of 1 M HCl. After an incubation time of 10 min, 4 ml of 1 M NaOH were added and extinction at 320 nm was measured against H_2O. To exclude absorbance caused by the uncatalyzed rearrangement of chorismate, blanks of increasing chorismate concentrations without enzyme were prepared and absorbance was measured. These blank absorbances were subtracted from optical densities measured for enzyme activities. A calibration curve was drawn using different known phenylpyruvate concentrations that were treated the same way as the enzyme reactions. The molecular extinction coefficient at 30 °C was determined as 13095 $M^{-1}\ cm^{-1}$. For determination of the pH optima, a universal buffer solution with a pH range of 2.5–12 containing 30 mM citric acid, 30 mM KH_2PO_4, 30 mM H_3BO_4, 30 mM diethylbarbituric acid and different amounts of NaOH was used.

The collected data were transformed to international units (μmol min^{-1}) per mg of enzyme. The maximum velocity V_{max}, the Hill-coefficient n_H, and the substrate concentration at half-maximal velocity $[S]_{0.5}$ or K_m were determined using a computer program which applied the Quasi-Newton method (Davidon-Fletcher-Powell algorithm) to fit optimal curves to the data (31). To draw substrate saturation curves, the data were fitted either to the Michaelis-Menten equation ($v = V_{max}\ [S]\ (K_m + [S])^{-1}$) or to the Hill equation ($v = V_{max}\ [S]^n\ ([S]^n + S')^{-1}$), where $S'^{(1/n)} = S_{0.5}$. Eadie-Hofstee plots ($v\ [S]^{-1}$ *versus* v) were drawn to decide which equation a set of kinetic data had to be applied. Enzyme kinetics without cooperativity result in a linear curve, whereas even small degrees of cooperativity result in concave curvatures of the kinetic data (32). Hill plots ($\log(v\ (V_{max} - v)^{-1})$ *versus* log [S]) were used to calculate Hill coefficients. The resulting V_{max} values were transformed to catalytic constants ($k_{cat} = V_{max}\ M_r\ E_0^{-1}$ (60 s)$^{-1}$; substrate turnover per active site). The inhibitor constant K_i for tyrosine was determined according to Dixon by plotting v^{-1} *versus* inhibitor concentration (33).

Determination of the Native Molecular Weight—The native molecular weight of the chorismate mutase was estimated by gel filtration on a Superdex 200 prep grade column using 50 mM potassium phosphate, 150 mM NaCl, pH 7.6, as elution buffer. The void volume of the column was determined with blue dextran and a calibration plot was defined using a gel filtration chromatography standard from Bio-Rad containing thyroglobulin, bovine γ-globulin, chicken ovalbumin, equine myoglobin, and vitamin B-12. In addition, the molecular weight was determined independently by sedimentation equilibrium at 50,000 rpm (16 °C) and calculation of the sedimentation coefficient and the molecular mass. Three different concentrations of the enzyme in 20 mM potassium phosphate buffer, pH 7.6, were used and all ultracentrifugal analyses were performed on a Beckmann XLA. To confirm the results obtained by gel filtration and analytical ultracentrifugation, the molecular weight was estimated by native polyacrylamide gel electrophoresis using a gradient from 4 to 20% polyacrylamide (34).

Determination of the Isoelectric Point—The isoelectric point of the chorismate mutase enzyme was determined using the Bio-Rad Rotofor system according to the supplier's instructions. A pH gradient in 18 ml of 10 mM potassium phosphate buffer, pH 7.6, was set up by a Bio-Lyte™ ampholyte ranging from pH 3.5 to 9.5 in a concentration of 0.5%. 100 μg of purified protein were applied to the focusing chamber and after 4 h the run was completed. The content of the focusing chamber was fractionated and the pH of each fraction was measured. Before detection of chorismate mutase, NaCl was applied to 1 M final concentration and fractions were dialyzed against 10 mM potassium phosphate, pH 7.6. Chorismate mutase was detected by enzyme assays as well as by SDS-polyacrylamide gel electrophoresis.

Electron Microscopy—Negative staining of protein samples was performed as described in Ref. 35 with 4% uranyl acetate solution. Electron microscopic images were taken at a EM 301 transmission electron microscope (Philips, Eindhoven, Netherlands) at an acceleration potential of 80 kV. Magnification was calibrated using a cross-grid replica.

Western Blot Analysis—Immunological detection of chorismate mutase proteins was performed using a polyclonal rabbit antibody raised against purified yeast chorismate mutase (10) and a second antibody with horseradish peroxidase activity. Detection was carried out using the ECL method (36).

Sequence Alignment and Homology Modeling Studies—All sequence analyses were performed using the LASERGENE Biocomputing software from DNAstar (Madison, WC). Alignments were created based on the Lipman-Pearson method (37). For homology modeling, the deduced primary structure of the *A. nidulans* chorismate mutase was aligned to the crystallographic data of yeast chorismate mutases as described in the Brookhaven protein data base (12) by ProModII (38) and refined by the SWISS-MODEL service (39, 40). Using the MOLMOL software (41), a three-dimensional structure model could be established by calculation of secondary structures.

[1] The abbreviations used are: kb, kilobase(s); bp, base pair(s).

```
              v10       v20       v30       v40       v50
AnCM MDTAIDLSDASKALDLANIRFQLIRLEDTITFHLIERVQFPLNKTIYIPG--GV
       :|::.:...|:|.||| :|:|:|||:|.|.:||| :|:   ::| :.  |:
ScCM     MDFTKPETVLNLQNIRDELVRMEDSIIFKFIERSHFATCPSVYEANHPGL
                ^10       ^20       ^30       ^40       ^50

              v60       v70       v80       v90       v100
AnCM KIPNEQISLMDYLLRETERLQSRVRRYQSPDEYPFFPSALEKPILQPLDY
      .||| : |::|. |.: |  :||:|||::|||| |||||. ::|::|.:::|
ScCM EIPNFKGSFLDWALSNLEIAHSRIRRFESPDETPFFPDKIQKSFLPSINY
               ^60       ^70       ^80       ^90       ^100

              v110      v120      v130      v140      v150
AnCM PKIL--HDNDVNVNETIKTRYVQDILPAICPQFGGREDRGETQENYGSAA
      |:||  .. :|| |:.||. |::.|:| |     :: | |:.::|:||.|
ScCM PQILAPYAPEVNYNDKIKKVYIEKIIPLI-----SKRD-GDDKNNFGSVA
               ^110      ^120           ^130       ^140

              v160      v170      v180      v190      v200
AnCM TCDVSCLQALSRRIHFGKFVAESKFQKETEKFVALIKAGDRKEIDEAITD
      | |:.|||:|||||||||||||:|||.:.  :. |||: | ..| ..||:
ScCM TRDIECLQSLSRRIHFGKFVAEAKFQSDIPLYTKLIKSKDVEGIMKNITN
          ^150      ^160      ^170      ^180      ^190

              v210      v220      v230      v240      v250
AnCM AKVEQKVLERLALKAKTYGTDPGFPEQSGPKIDVQAVQDMYKEYVIPLTK
      : ||:|:||||: ||..||.||.  | :..:|. : : .:||| |||:||
ScCM SAVEEKILERLTKKAEVYGVDPT-NESGERRITPEYLVKIYKEIVIPITK
          ^200      ^210       ^220      ^230      ^240

              v260
AnCM VVEVEYLMQRLKGTQWE
       ||||||::||..
ScCM EVEVEYLLRRLEE
          ^250
```

FIG. 1. **The chorismate mutase of *A. nidulans* shows homology to the *S. cerevisiae* enzyme.** The alignment shows a comparison of the deduced amino acid sequence of *A. nidulans* chorismate mutase (*AnCM*) with that of *S. cerevisiae* (*ScCM*). Identical residues are indicated by *vertical bars*, conservative replacements by *colons*, and neutral changes by *periods*.

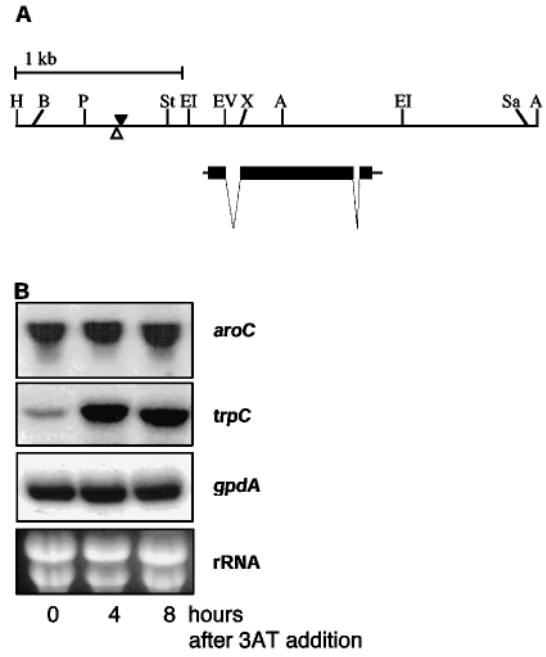

FIG. 2. **Structure of the *aroC* gene and expression under amino acid starvation conditions.** *A*, schematic drawing of a genomic *Hin*dIII/*Aat*II DNA fragment containing the *aroC* gene. The GenBank accession number for this sequence is AF133241. *Solid boxes* indicate the open reading frame interrupted by two introns. A putative STUA-binding site is indicated by the *solid triangle* and a Gcn4p response element in reverse orientation by the *open triangle*. *A*, *Aat*II; *B*, *Bst*EII; *EI*, *Eco*RI; *EV*, *Eco*RV; *H*, *Hin*dIII; *P*, *Pvu*II; *Sa*, *Sal*I; *St*, *Stu*I; *X*, *Xba*I. *B*, Northern analysis of total RNA prepared from *A. nidulans* strain FGSC A234 (*yA2*, *pabaA1*, *veA1*) different time points after shifting to medium containing 3-amino-1,2,4-triazole (*3AT*). Each lane was loaded with 20 μg of total RNA and probed successively with probes specific for *aroC*, *trpC*, and *gpdA*. Ethidium bromide-stained total RNA is included as control.

RESULTS

Isolation of the aroC Gene from A. nidulans—The *aroC* gene from *A. nidulans* was cloned by functional complementation of a *S. cerevisiae aro7*Δ mutant strain (10). Yeast strains with a deleted *ARO7* gene do not contain any chorismate mutase activity and therefore were unable to grow on minimal medium lacking tyrosine or phenylalanine. Yeast strain RH2185 (*aro7::LEU2*, *ura3–52*) was transformed with *A. nidulans* cDNA expressed from the *GAL1* promoter (18) and transformants were selected by growth on medium lacking tyrosine and phenylalanine containing 2% galactose as the sole carbon source. A total of 80 colonies were obtained, from which plasmids were isolated that could complement the Phe/Tyr auxotrophy of the recipient *aro7*Δ yeast strain. One of the plasmids (pME1498) was further analyzed by DNA sequencing of the *Sal*I/*Not*I fragment containing the cDNA insert. The cDNA without poly(A) tail is 927 bp in length and includes an open reading frame of 804 bp with 267 codons which correspond to a polypeptide with a calculated M_r of 30,660. Alignment of the deduced amino acid sequence shows strong homology to the chorismate mutase sequence of *S. cerevisiae* with 44% identity (Fig. 1). The homology goes up to 67% when conservative changes are taken into account.

The genomic region encoding the cDNA insert of pME1498 was isolated and analyzed. Southern blot analysis of this region, using the cDNA of pME1498 as a probe, revealed that the corresponding gene exists as single copy in the *A. nidulans* genome (data not shown). A sublibrary of *A. nidulans* genomic *Hin*dIII fragments of 4–6 kb in size was screened by colony hybridization with the *aroC* cDNA probe and resulted in a 5-kb fragment which was subjected to DNA sequence analyses (Fig. 2*A*). The genomic fragment contains the same open reading frame as the cDNA, flanked by a 1.2-kb 5′-region and a 2.7-kb 3′-region, and is interrupted by two short intron sequences. Intron I is located 70 bp downstream of the translational start site and is 113 bp in length, while intron II is located 77 bp upstream of the stop codon UAG and 49 bp in size. Both show the conserved 5′ splicing, internal, and 3′ splicing sequences described for *A. nidulans* introns (42). Sequence analysis for upstream regulatory sequences in the promoter region of *aroC* indicated a putative STUA-binding site 560 nucleotides upstream of the translational start codon. This sequence element (5′-ACGCGAAA-3′) matches the described consensus for STUA response elements (StRE, 5′-(A/T)CGCG(T/A)N(A/C)-3′) (43). In addition, a sequence element (5′-GAGTCA-3′) was identified 571 bp upstream of the translational start codon that matches the described consensus sequence for a Gcn4p-binding site (GCRE, 5′-TGACTC-3′) in reverse orientation (44).

A. nidulans mutant strains auxotrophic for phenylalanine and tyrosine have been isolated before (23). One complementation class of these mutants was named *aroC* and mapped to linkage group I (45). The described phenotype of *aroC* mutant strains prompted us to test whether the gene isolated was able to complement the auxotrophy of *aroC* mutants. For this purpose, the genomic *Hin*dIII fragment was transformed into strain G1100 (*aroC1248, riboA1, adG14, yA2*) for ectopic integration and transformants were selected on medium lacking phenylalanine and tyrosine. For 90% of the isolated transformants a complementation of the Phe/Tyr auxotrophy was observed, indicating that we had isolated the *aroC* gene of *A. nidulans*, which codes for the chorismate mutase enzyme.

aroC Expression Is Not Regulated Transcriptionally upon Amino Acid Starvation—By Northern blot analysis using an RNA size standard the transcript length of *aroC* was determined to be approximately 0.96 kb (not shown). As the *aroC* gene product is an enzyme of the aromatic amino acid biosyn-

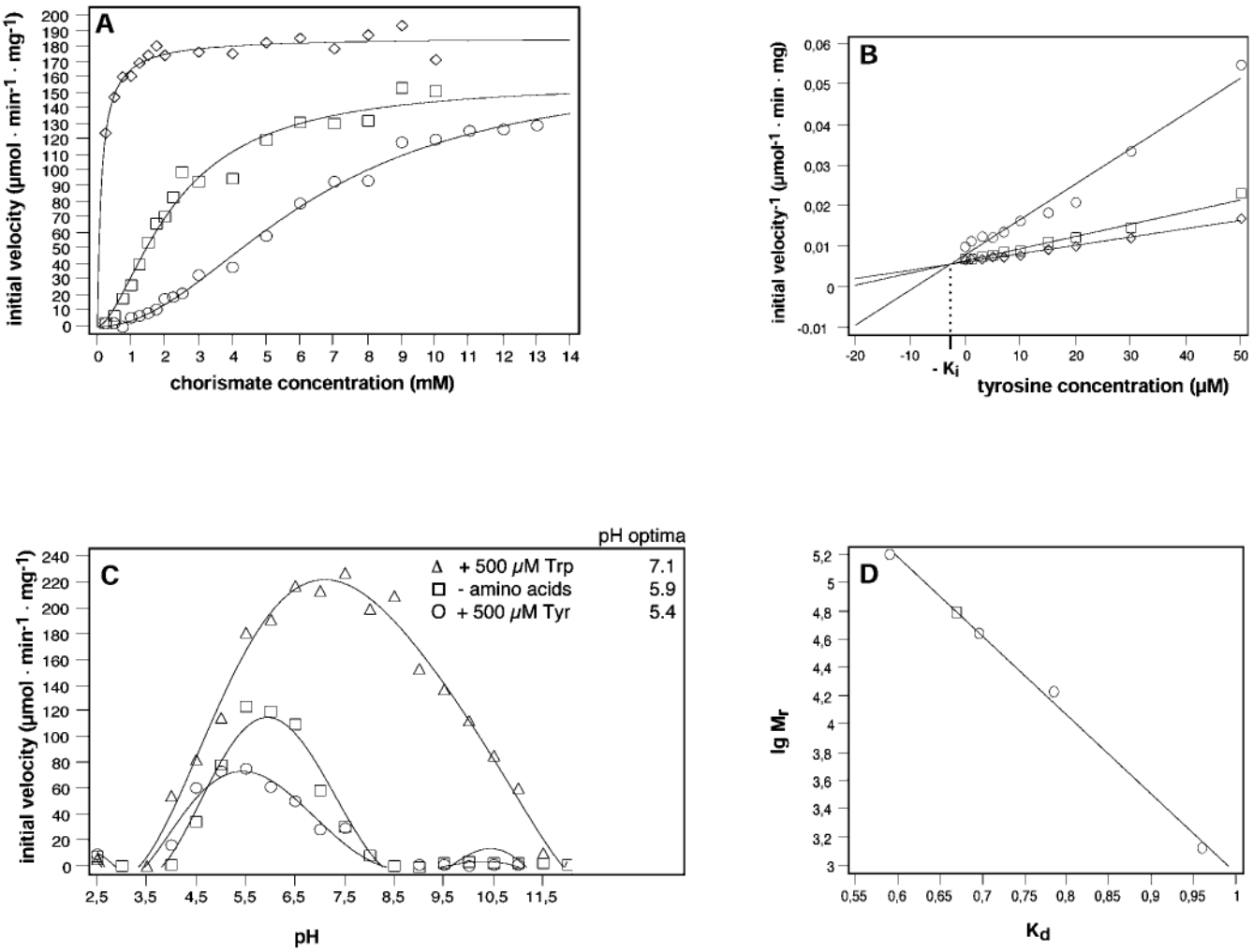

FIG. 3. **Characteristics of *A. nidulans* chorismate mutase.** *A*, substrate saturation plot of enzyme assays. The enzyme was assayed with 5 µM tryptophan (◇), without effector (□), or in the presence of 50 µM tyrosine (○). The data were fitted to functions describing cooperative or Michaelis-Menten-type saturation. Specific activities are mean values of five independent measurements with a standard deviation not exceeding 20%. *B*, Dixon plot of enzyme assays in the presence of tyrosine at different concentrations. Specific activities were measured in the presence of 2 mM (◇), 3 mM (□), and 4 mM (○) substrate and plotted reciprocally *versus* tyrosine concentrations. The point of intersection determines the inhibitory constant K_i for tyrosine. *C*, pH optima for chorismate mutase activities under different effector conditions at 1 mM chorismate concentration. The optima are given on the right side. *D*, determination of native molecular weight by gel filtration. Calibration of a Superdex 200 column was performed as described under "Experimental Procedures." Using a void volume of 47.19 ml as determined by blue dextran and a total column volume of 120 ml, the K_d of the native chorismate mutase (□) was calculated to be 0.67. This value corresponds to a polypeptide with an apparent molecular mass of 62,187 Da.

thetic pathway and because of the existence of a putative GCRE in its promoter region we were interested in whether *aroC* expression is affected by amino acid starvation conditions. For that purpose, *A. nidulans* strain FGSC A234 (*yA2*, *pabaA1*, *veA1*) was cultivated in liquid minimal medium for 20 h and mycelia were transferred to fresh medium containing 3-amino-1,2,4-triazole (3AT). This reagent acts as false feedback-inhibitor on the histidine biosynthesis and therefore mimics amino acid starvation by depletion of the histidine pool within the fungus (46). After different time points mycelium was harvested and total RNA was prepared. Following Northern blot the *aroC* transcript levels were determined by probing with the cDNA fragment. Additionally, the levels of the *gpdA* (47) and the *trpC* (48) transcripts were detected with specific probes serving as internal controls (Fig. 2B). *gpdA*, which encodes an enzyme of glycolysis (glyceraldehyde-3-phosphate dehydrogenase, EC 1.2.1.12), is known to be unregulated in its transcription upon 3-amino-1,2,4-triazole addition. In contrast, *trpC*, which codes for a trifunctional enzyme of tryptophan biosynthesis, has been shown to be transcriptionally regulated by amino acid starvation conditions. Quantification of signal strength reveals constant expression of *aroC* after shifting to amino acid starvation conditions. Expression of *gpdA* shows the identical pattern, whereas *trpC* transcription is increased by a factor of 15, 8 h after the onset of the environmental stimulus. Therefore we conclude that transcription of the *aroC* gene is not affected by a regulatory network that acts upon the environmental signal amino acid starvation.

Chorismate Mutase of A. nidulans Is Regulated by Tyrosine and Tryptophan—The enzyme was purified by overexpression in *S. cerevisiae* strain RH2192 (*aro7::LEU2, ura3-52*) from a high-copy plasmid carrying the *A. nidulans aroC* cDNA fragment driven by the *MET25* yeast promoter. The protein was enriched 64-fold and purified to homogeneity to determine the properties of the *aroC* gene product.

Kinetic stop assays with the unliganded enzyme were performed to reveal the catalytic properties of the *A. nidulans* chorismate mutase (Fig. 3*A*, Table I). In the absence of effectors the enzyme shows positive cooperativity toward its substrate chorismate leading to a sigmoidal substrate saturation curve. A $[S]_{0.5}$ value of 2.3 mM and a Hill coefficient n_H of 1.56 were determined and the maximal turnover rate k_{cat} was calculated

TABLE I

Kinetic parameters of chorismate mutase enzyme from A. nidulans

Values for k_{cat}, K_m, and $[S]_{0.5}$ were defined by fitting initial velocity data to equations describing hyperbolic or cooperative saturation, respectively. Hill coefficients (n_H) were calculated from Hill plots by linear regression.

	Inhibited (50 μM tyrosine)			Unliganded			Activated (5 μM tryptophan)		
	k_{cat}	$[S]_{0.5}$	n_H	k_{cat}	$[S]_{0.5}$	n_H	k_{cat}	K_m	n_H
	s^{-1}	mM		s^{-1}	mM		s^{-1}	mM	
	82.5	6.4	1.69	82	2.3	1.56	92	0.1	0.95
k_{cat}/K_m ($mM^{-1} \cdot s^{-1}$)		12.9			35.7			920	

to be 82 s^{-1} per active site. By isoelectric focusing, the pI of the protein was determined to be at an acidic pH of 4.7 (data not shown). The solvent pH also has an influence on the catalytic activity of the enzyme (Fig. 3*C*). Without any effector bound, chorismate mutase activity reaches its maximum at a pH of 5.9.

To reveal the regulatory behavior of the enzyme, kinetic assays were performed in the presence of allosteric effectors (Fig. 3*A*, Table I). Tryptophan at 5 μM concentration has a strong effect on the catalytic rate. Cooperativity is lost (n_H = 0.95), leading to a Michaelis-Menten-type kinetic with a K_m of 0.1 mM and the maximal turnover number is increased to 92 s^{-1}. In contrast, tyrosine acts as inhibitor of chorismate mutase activity. 50 μM of this amino acid resulted in a $[S]_{0.5}$ value of 6.4 mM with a turnover rate of 82.5 s^{-1}. The Hill coefficient of 1.69 indicates the retained cooperativity. The influence of tyrosine was further examined by kinetic assays in the presence of different amounts of this effector. Evaluation of these data according to Dixon (33) leads to a set of linear curves, one for each chorismate concentration (Fig. 3*B*). The point of intersection reveals an inhibitory constant K_i of 2.8 μM and further indicates the type of mixed inhibition. In summary, chorismate mutase of *A. nidulans* is tightly regulated in its catalytic activity by tryptophan and tyrosine, with tryptophan as positive effector having a stronger influence on enzymatic behavior. This is indicated by the fact that alteration of enzyme kinetics is achieved at 10-fold lower concentration (5 μM) compared with the inhibitory concentration of tyrosine (50 μM). The allosteric effectors also show an influence on enzymatic activity with respect to solvent pH (Fig. 3*C*). Tyrosine shifts the catalytic maximum to a value of 5.4, whereas in the presence of tryptophan maximal catalytic activity is achieved at pH 7.1. In addition, tryptophan broadens the pH range of detectable catalytic activity.

The Chorismate Mutase of A. nidulans Is a Dimer—In order to elucidate the quaternary structure of the *aroC* gene product, different approaches were carried out. By analytical ultracentrifugation a mean sedimentation constant S of 4.35 ± 0.2 was determined (data not shown). Using a calculated molecular mass of 30.0 kDa for one single chorismate mutase polypeptide, this S value indicates the existence of a homodimeric structure. Gel filtration analysis supports this result (Fig. 3*D*). The purified protein eluted from a calibrated Superdex 200 column at a defined elution volume corresponding to a K_d value of 0.67. This value matches the estimated K_d for a protein of 62.2 kDa, therefore the chorismate mutase had passed the column as a dimer. Additionally, gradient polyacrylamide gel electrophoresis under nondenaturing conditions indicated an apparent molecular mass of the native enzyme of approximately 65 kDa (data not shown).

To analyze the structure of AROC, electron microscopic images of the purified enzyme were taken at a magnification of 1:3.1 × 10^5 (Fig. 4*A*). The images show the presence of a globular protein, approximately 13 × 7 nm in size. Different projections of the protein show a cleft between two subunits, indicating a structure where two identical subunits are connected by a dimeric interface.

Antibodies against the Yeast Chorismate Mutase Recognize the A. nidulans Enzyme—Given the globular, homodimeric structure of the chorismate mutase from *A. nidulans* and its similarity in the deduced amino acid sequence to the yeast enzyme, we performed molecular modeling studies based on the homology to known crystal structures. A three-dimensional structure of the *A. nidulans* enzyme was deduced on the basis of the crystal structures of the yeast chorismate mutases and the secondary structure elements of this newly created structure were calculated. The proposed three-dimensional structure of the enzyme from *A. nidulans* shows an all-helical structure (Fig. 4*B*) consisting of 12 helices which resembles that of the yeast protein. Superposition of both structures points out the similarity between them which is highest for the helical elements. Differences between the structures exist in the loops that connect these helices, especially for the loop preceding helix 12 (loop220s).

The modeling studies suggest that similar epitopes exist on the *A. nidulans* chorismate mutase in comparison to the yeast enzyme. To test this hypothesis, we performed immunoblotting with a polyclonal rabbit antibody raised against purified yeast chorismate mutase. Western blots of cell extracts of yeast strain RH2192 harboring the coding cDNA for *aroC* or the *ARO7* gene of *S. cerevisiae*, respectively, on a 2-μm overexpression plasmid revealed a high affinity of this antibody to the *A. nidulans* enzyme (Fig. 4*C*). Therefore, we conclude that similar epitopes exist on both chorismate mutases and that the structure of the *A. nidulans* enzyme resembles that of the yeast protein.

A Crucial Region for Allosteric Regulation of the Yeast Enzyme Is Not Conserved in the A. nidulans Chorismate Mutase—Given the strong homology of the *aroC* gene product to yeast chorismate mutase, we were interested in whether the mechanism of allosteric transition is conserved in these related proteins. For the Aro7p of *S. cerevisiae*, it has been shown that a single threonine residue in loop220s (Thr^{226}) is important for proper signal transduction from the effector binding sites to the catalytic centers of the homodimer (14). Exchange of that amino acid residue to isoleucine (*ARO7*^{T226I}) leads to a constitutively activated enzyme that is locked in the *R* state. Upon alignment of the primary structures of AROC and Aro7p, an aspartate residue (Asp^{233}) corresponds to that position in the *A. nidulans* enzyme (Fig. 1*B*). By site-directed mutagenesis, this residue was changed to threonine and isoleucine, respectively, in the *aroC* gene product. Both alleles (*aroC*^{D233T}, *aroC*^{D233I}) were able to complement the yeast *aro7*Δ deletion indicating that they are expressed properly in the recipient strain. After overexpression in the yeast *aro7*Δ mutant strain RH2192, desalted crude extracts were prepared and specific chorismate mutase activities were determined in the absence or presence of effectors, respectively. In addition, the corresponding *ARO7* alleles, *ARO7*^{wt}, *ARO7*^{T226I}, and *ARO7*^{T226D}, were expressed from the same plasmid in the *aro7*Δ strain and the specific activities were determined in desalted crude extracts under identical conditions (Table II).

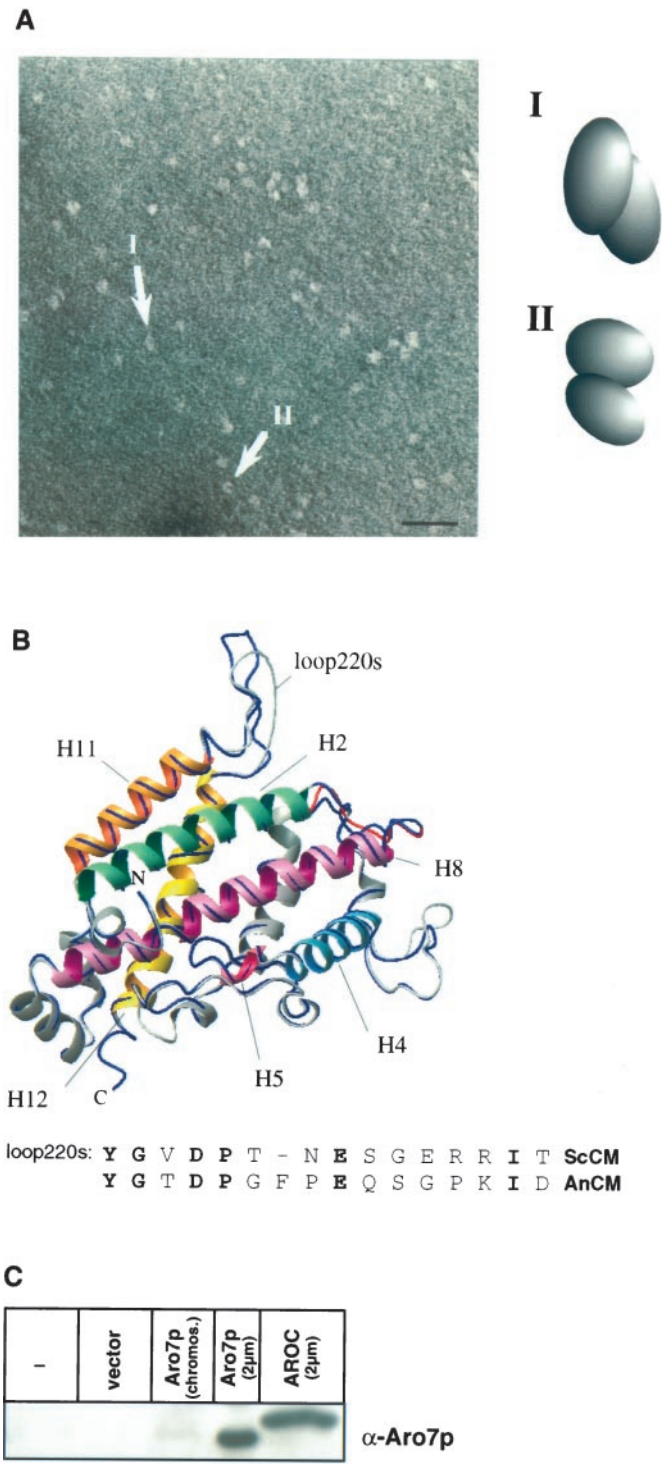

FIG. 4. **The *A. nidulans* chorismate mutase shares structural similarities with its yeast homologue and is bound with high affinity by a polyclonal antibody against the yeast enzyme.** *A*, electron microscopy images show a globular tertiary structure of chorismate mutase built up by two spherical subunits. Pictures of the purified protein were taken at 3.1×10^5-fold magnification. *Arrows* point out two molecules for which schematic models are shown on the *right side*. *Scale bar* equals 32 nm. *B*, homology modeling of *A. nidulans* chorismate mutase based on crystal structures of the yeast enzyme. The primary sequence of the *aroC* gene product was modeled on known three-dimensional structures of yeast chorismate mutase monomers by SWISS-MODEL. In the superimposition the tertiary structure of the yeast protein is represented as *gray ribbons*, structures of AROC are indicated as a *black line*. *C* indicates the C terminus of the protein, *N* its N terminus. Important helices (*H*) are indicated as well as loop220s connecting helix 11 and 12. The alignment shows a section of both enzymes compromising the region of loop220s with identical residues in **bold**. *C*, a polyclonal rabbit antibody raised against yeast chorismate mutase binds the AROC enzyme with high affinity. The immunoblot shows 15 μg of crude extracts of yeast strain RH2192 (*aro7::LEU2*) harboring different 2-μm expression plasmids. *Lane 3* contains crude extract from yeast strain RH2191 carrying one chromosomal copy of the *ARO7* gene. Proteins cross-reacting with polyclonal antiserum raised against purified yeast chorismate mutase were detected using enhanced chemiluminescence.

TABLE II

Specific enzyme activities of mutant chorismate mutases

Catalytic activities were determined in desalted crude extracts of yeast strain RH2192 expressing different chorismate mutase-encoding alleles on a 2-μm overexpression plasmid driven by the *MET25* promoter. The values measured for each enzyme were standardized for plasmid copy number by Southern analyses.

Protein	Specific activity[a] (nmol · min^{-1} mg^{-1})			Range of modulation
	Unliganded	Inhibited	Activated	
AROC	32.5	8.4	88.5	11
AROC^{D233I}	30.3	13.4	63.0	4.7
AROC^{D233T}	41.3	22.0	64.3	2.9
Aro7p	4.8	1.2	40.2	34
Aro7^{T226I}p	20.6	21.7	26.4	1.3
Aro7^{T226D}p	3.7	3.3	11.1	3.4

[a] Assay conditions were 50 μg of total protein and 2 mM chorismate, 3-min reaction time, and 100 μM tyrosine or 500 μM tryptophan, respectively. Each value is the mean of three independent measurements with a standard deviation not exceeding 20%.

Generally, the *A. nidulans* chorismate mutase enzymes showed higher specific activities in these assays than their yeast homologues. For the AROC wild-type enzyme a specific activity of 32.5 units/mg of total protein was measured, which is repressed 3.9-fold to 8.4 units mg^{-1} in the presence of 100 μM tyrosine, whereas tryptophan at 500 μM concentration leads to a 2.7-fold increase in specific activity to a value of 88.5 units mg^{-1}. In contrast, yeast chorismate mutase activity expressed from the *ARO7*^{T226D} allele was measured to be 3.7 units mg^{-1}. In its inhibited form the enzyme is slightly repressed in its activity (3.3 units mg^{-1}). In the presence of tryptophan, activity is increased 3-fold to 11.1 units mg^{-1}. The proteins with a substitution to isoleucine clearly differ in their enzymatic properties. The unliganded *aroC*^{D233I} gene product shows a specific activity of 30.3 units mg^{-1}, which is repressed 2.3-fold when liganded by tyrosine (13.4 units mg^{-1}) and increased 2.1-fold to 63.0 units mg^{-1} by its activator tryptophan. The yeast counterpart Aro7^{T226I}p has a specific activity of 20.6 units mg^{-1} and shows almost no regulatory response to both effectors which is characteristic for this constitutively activated enzyme. Substitution of residue 233 in the *A. nidulans* enzyme to threonine leads to a chorismate mutase with a reduced regulatory range. The uneffected enzymatic activity of 41.3 units mg^{-1} is decreased 1.9-fold to 22.0 units mg^{-1} by tyrosine and increased 1.6-fold to 64.3 units mg^{-1} by tryptophan. The corresponding wt-Aro7p enzyme shows a specific activity of 4.8 units mg^{-1} in its unliganded state. This value is decreased 4-fold to 1.2 units mg^{-1} in the presence of tyrosine, whereas tryptophan leads to a 8.4-fold increase of specific activity to 40.2 units/mg of protein.

In summary, both AROC mutant proteins exhibit a reduced range of regulatory properties in comparison to the wild-type enzyme. In the wild-type enzyme, carrying the charged amino acid aspartate at position 233, modulation of chorismate mutase activity by the heterotropic effectors tyrosine and tryptophan, respectively, is given by a factor of 11. In the protein derived from the *aroC*^{D233I} mutant allele, the substitution to an apolar amino acid residue leads to reduced modulation and enzymatic activity is within a range of 5. The AROC^{D233T}

protein shows almost no response to the effectors with a narrow window of regulation by a factor of 3. The exchange of the aspartate residue to the polar amino acid threonine therefore seems to disturb the intramolecular signal transduction pathway for the allosteric switch.

Taken together, the data clearly show that the chorismate mutase enzymes of the bakers' yeast and the filamentous fungus *A. nidulans* share regulatory and structural properties. Despite these similarities the intramolecular signal transduction pathway for allosteric transition as proposed for the yeast enzyme seems to be not conserved in the AROC protein.

DISCUSSION

The metabolic pathway of aromatic amino acid biosynthesis is a conserved reaction cascade converting two compounds of primary metabolism to phenylalanine, tyrosine, and tryptophan. The flux of compounds through this pathway has to be strictly regulated as synthesis of aromatic amino acids is an energy-consuming process. One mode of regulation lies in controlling the activity of branch point enzymes within a pathway, either by altering their catalytic properties or via altered enzyme levels within a cell. In the aromatic amino acid biosynthetic pathway, the chorismate mutase enzyme is one major point of attack in regulating the flux of chorismic acid into the tyrosine/phenylalanine-specific branch.

We have demonstrated that the protein specified by the *aroC* gene of *A. nidulans* is the chorismate mutase enzyme of this filamentous fungus. According to its high sequence similarity to the monofunctional chorismate mutase of *S. cerevisiae* the *A. nidulans* enzyme has to be classified as a member of the AroQ class of chorismate mutases. The kinetic properties of this enzyme demonstrate that the *aroC* gene product is tightly regulated in its activity. The substrate, chorismate, serves as homotropic, positive effector as deduced from positive cooperativity in substrate saturation assays. The determined Hill coefficient of 1.56 clearly indicates that the enzyme contains at least two substrate-binding sites. In addition, two aromatic amino acids show heterotropic effects on enzymatic activity. Tyrosine, one end product of the chorismate mutase-specific branch, influences catalytic efficiency negatively, whereas tryptophan, the end product of the opposite branch, strongly increases catalytic turnover. Therefore this chorismate mutase enzyme fits well in the model of allosterism as established by Monod and co-workers (49). In this simple model a given enzyme exists in two (or more) structural states, tense (*T*-) or relaxed (*R*-), with different catalytic activities. The equilibrium between these states is changed upon substrate binding to the active site or by binding of inhibitory or activating ligands at distinct allosteric sites. Further reference to allosterism is given by the homodimeric structure of the *A. nidulans* chorismate mutase since allosteric enzymes are often multimeric proteins.

pH dependence of catalytic activity of the chorismate mutase from *A. nidulans* shows three distinct optima. For the unliganded enzyme the pH optimum of 5.9 fits quite well the intracellular pH in filamentous fungi, which is in a range of 5.7 to 6.5 (50). The negative effector tyrosine shifts this optimum only slightly to a value of 5.4, whereas tryptophan alters the range of catalytic activity dramatically: maximum turnover is achieved at the neutral pH of 7.1 and catalytic activity is present over a pH range between 4 and 12. This pH-dependent catalytic behavior is contrary to that known from bacterial chorismate mutases where highest catalytic activities are achieved at alkaline pH (51, 52). On the other hand the catalytic activities of the *A. nidulans* enzyme at different pH values resemble that of yeast chorismate mutase. For the *A. nidulans* chorismate mutase, similar absolute catalytic activities were determined as described for the yeast enzyme (10). Without any effector present, enzymatic activity was measured over 4.5 pH units and tyrosine restricted catalytic activity to a range of 3 pH units (Fig. 3*C*). One difference concerning pH dependence is the range of detectable catalytic activity in the presence of tryptophan. The heterotropic positive effector broadens the pH range of activity to 8 pH units compared with a value of 6 units as reported for the *S. cerevisiae* enzyme. In the yeast protein the active site residue Glu^{246} has been identified to be important in restricting enzyme activity to acidic conditions (10). Upon alignment, this particular residue is conserved within the primary structure of the *A. nidulans* enzyme (Glu^{253}).

In yeast chorismate mutase, different domains within the dimeric structure have been identified (53). Upon effector binding, the two subunits rotate relative to each other and the allosteric signal is transmitted toward the polypeptide to the catalytic domain. The dimeric structure and all specific amino acids of the yeast enzyme which are important for binding of effectors (Arg^{75}, Arg^{76}, Asn^{139}, Ser^{142}, and Thr^{145}) and allosteric signal transduction (Glu^{23}, Asp^{24}, Phe^{28}, and Tyr^{234}), as well as active site residues (Arg^{16}, Arg^{157}, Lys^{168}, Glu^{198}, and Thr^{242}) are conserved in the chorismate mutase of *A. nidulans* (Fig. 1*B*). Additionally, *in silico* studies showed that AROC can be modeled quite closely onto the tertiary structure of the yeast protein. Therefore, it was surprising that one particular residue, Thr^{226}, of the yeast enzyme is not conserved in its *A. nidulans* counterpart, as this residue had been characterized as the molecular switch in transmitting the signal for *T* to *R* state transition (9). By site-directed mutagenesis we created two mutant AROC enzymes. None of these enzymes turned out to be locked in either allosteric state, but both proteins showed decreased regulatory properties upon effector binding. We conclude that this narrow window of regulatory modulation represents intermediate states between tense and relaxed state. The role of loop220s in transmitting the intramolecular signal from the effector binding sites to the catalytic domains is obviously different in the chorismate mutases of *S. cerevisiae* and *A. nidulans*. Whereas in the yeast protein substitution of one particular residue in loop220s locks the whole enzyme in its activated state, we did not find such a behavior in the AROC mutant enzymes. Taking into account that the *A. nidulans* enzyme resembles its yeast homologue with respect to catalytic and regulatory behavior as well as structural properties this difference is surprising. It implicates that the structure of this loop preceding helix 12, which is part of the catalytic domain, is more flexible in the *A. nidulans* enzyme than in the yeast chorismate mutase. Additionally, we suggest that alternative pathways within the molecule could exist for signal transduction to the active site in contrast to one exclusive via loop220s.

Allosterism is one possible way in regulating enzymatic activity. In living systems additional mechanisms of flux control through a metabolic pathway exist which affect the rate of expression of a given enzyme. For the *aroC* gene product data indicate that its expression is not regulated transcriptionally via the cross-pathway control network (54). Amino acid starvation conditions showed no influence on *aroC* transcript levels which is consistent with data obtained for *S. cerevisiae* (55). Sequence analysis for upstream regulatory sequences indicated a putative STUA-binding site 560 nucleotides upstream of the translational start codon of *aroC*. This sequence element matches the described consensus for STUA response elements (42). As a filamentous fungus *A. nidulans* has developed additional regulatory networks that constitute differentiation processes. Preliminary transcript level analyses indicate that *aroC* expression is down-regulated drastically after the developmental program of asexual conidiation is initiated (not shown).

Future research will have to identify *trans* factors as well as *cis* elements responsible for this type of regulation and elucidate whether this is specific for chorismate mutase expression or, in contrast, is a general effect after the developmental program has been established.

Acknowledgments—We thank Gaby Heinrich for support in the initial phase, Dr. Hans-Ulrich Mösch for critical reading of the manuscript, and all other members of the laboratory for helpful discussions. We also thank Dr. Christian Urbanke, Hannover, for determining the native molecular weight on an ultracentrifuge.

REFERENCES

1. Weiss, U., and Edwards, J. M. (1980) *The Biosynthesis of Aromatic Amino Acids,* Wiley, New York
2. Braus, G. H. (1991) *Microbiol. Rev.* **55,** 349–370
3. Andrews, P. R., Smith, G. D., and Young, I. G. (1973) *Biochemistry* **12,** 3492–3498
4. Romero, R. M., Roberts, M. F., and Phillipson, J. D. (1995) *Phytochemistry* **40,** 1015–1025
5. Chook, Y. M., Ke, H., and Lipscomb, W. N. (1993) *Proc. Natl. Acad. Sci. U. S. A.* **90,** 8600–8603
6. Chook, Y. M., Gray, J. V., Ke, H., and Lipscomb, W. N. (1994) *J. Mol. Biol.* **240,** 476–500
7. Gu, W., Williams, D. S., Aldrich, H. C., Xie, G., Gabriel, D. W., and Jensen, R. A. (1997) *Microb. Comp. Genomics* **2,** 141–158
8. MacBeath, G., Kast, P., and Hilvert, D. (1998) *Biochemistry* **37,** 10062–10073
9. Schmidheini, T., Sperisen, P., Paravicini, G., Hütter, R., and Braus, G. (1989) *J. Bacteriol.* **171,** 1245–1253
10. Schnappauf, G., Sträter, N., Lipscomb, W. N., and Braus, G. H. (1997) *Proc. Natl. Acad. Sci. U. S. A.* **94,** 8491–8496
11. Schnappauf, G., Krappmann, S., and Braus, G. H. (1998) *J. Biol. Chem.* **273,** 17012–17017
12. Sträter, N., Schnappauf, G., Braus, G. H., and Lipscomb, W. N. (1997) *Stucture* **5,** 1437–1452
13. Ma, J., Zheng, X., Schnappauf, G., Braus, G., Karplus, M., and Lipscomb, W. N. (1998) *Proc. Natl. Acad. Sci. U. S. A.* **95,** 14640–14645
14. Schmidheini, T., Mösch, H.-U., Evans, J. N. S., and Braus, G. (1990) *Biochemistry* **29,** 3660–3668
15. Martinelli, S. D., and Kinghorn, J. R. (eds) (1994) *Aspergillus, 50 Years on: Progress in Industrial Microbiology*, Elsevier Science B. V., Amsterdam
16. Adams, T. H., Wieser, J. K., and Yu, J.-H. (1998) *Microbiol. Mol. Biol. Rev.* **62,** 35–54
17. Dimroth, P. (1986) *Methods Enzymol.* **125,** 530–540
18. Liu, H., Krizek, J., and Bretscher, A. (1992) *Genetics* **132,** 665–673
19. Elble, R. (1992) *BioTechniques* **13,** 18–20
20. Punt, P. J., and van den Hondel, C. A. M. J. J. (1992) *Methods Enzymol.* **216,** 447–457
21. Mumberg, D., Müller, R., and Funk, M. (1994) *Nucleic Acids Res.* **22,** 5767–5768
22. Heinemeyer, W., Kleinschmidt, J. A., Saidowsky, J., Escher, C., and Wolf, D. H. (1991) *EMBO J.* **10,** 555–562
23. Roberts, C. F. (1969) *Aspergillus Newsletter* **10,** 19–21
24. Miozzari, G., Niederberger, P., and Hütter, R. (1978) *J. Bacteriol.* **134,** 48–59
25. Käfer, E. (1977) *Adv. Gen.* **19,** 33–131
26. Giebel, L. B., and Spritz, R. A. (1990) *Nucleic Acids Res.* **18,** 4947
27. Sanger, F., Nicklen, S., and Coulson, A. R. (1977) *Proc. Natl. Acad. Sci. U. S. A.* **74,** 5463–5467
28. Alwine, J. C., Kemp, D. J., and Stark, G. R. (1977) *Proc. Natl. Acad. Sci. U. S. A.* **74,** 5350–5354
29. Laemmli, U. K. (1970) *Nature* **227,** 680–685
30. Bradford, M. M. (1976) *Anal. Biochem.* **72,** 248–254
31. Fletcher, R., and Powell, M. J. D. (1963) *Computer J.* **6,** 163–168
32. Newell, J. O., and Schachmann, H. K. (1990) *Biophys. Chem.* **37,** 183–196
33. Dixon, M. (1953) *J. Biochem.* **55,** 170–171
34. Andersson, L. O., Borg, H., and Mikaelsson, M. (1972) *FEBS Lett.* **20,** 199–202
35. Valentine, R. C., Shapiro, P. M., and Stadtman, E. R. (1968) *Biochemistry* **7,** 2143–2152
36. Tesfaigzi, J., Smith-Harrison, W., and Carlson, D. M. (1994) *BioTechniques* **17,** 268–269
37. Lipman, D. J., and Pearson, W. R. (1985) *Science* **227,** 1435–41
38. Peitsch, M. C. (1996) *Biochem. Soc. Trans.* **24,** 274–279
39. Peitsch, M. C. (1995) *Bio/Technology* **13,** 658–660
40. Guex, N., and Peitsch, M. C. (1997) *Electrophoresis* **18,** 2714–2723
41. Koradi, R., Billeter, M., and Wüthrich, K. (1996) *J. Mol. Graph.* **14,** 51–55
42. May, G. S., Tsang, M. L.-S., Smith, H., Fidel, S., and Morris, N. R. (1987) *Gene (Amst.)* **55,** 231–243
43. Dutton, J. R., Johns, S., and Miller, B. L. (1997) *EMBO J.* **16,** 5710–5721
44. Hinnebusch, A. G. (1988) *Microbiol. Rev.* **52,** 248–273
45. Zaudy, G. (1969) *Aspergillus Newsletter* **10,** 22
46. Hilton, J. L., Kearney, P. C., and Ames, B. N. (1965) *Arch. Biochem. Biophys.* **112,** 544–547
47. Punt, P. J., Dingemanse, M. A., Jacobs-Meijsing, B. J. M., Pouwels, P. H., and van den Hondel, C. A. M. J. J. (1988) *Gene (Amst.)* **69,** 49–57
48. Yelton, M. M., Hamer, J. E., deSouza, E. R., Mullaney, E. J., and Timberlake, W. E. (1983) *Proc. Natl. Acad. Sci. U. S. A.* **80,** 7576–7580
49. Monod, J., Changeux, J. P., and Jacob, F. (1963) *J. Mol. Biol.* **6,** 306–329
50. Caddick, M. X., Brownlee, A. G., and Arst, H. N., Jr. (1986) *Mol. Gen. Genet.* **203,** 346–353
51. Schmit, J. C., and Zalkin, H. (1969) *Biochemistry* **8,** 174–181
52. Dopheide, T. A. A., Crewther, P., and Davidson, B. E. (1972) *J. Biol. Chem.* **247,** 4447–4452
53. Sträter, N., Håkansson, K., Schnappauf, G., Braus, G., and Lipscomb, W. N. (1996) *Proc. Natl. Acad. Sci. U. S. A.* **93,** 3330–3334
54. Piotrowska, M. (1980) *J. Gen. Microbiol.* **116,** 335–339
55. Schmidheini, T., Mösch, H.-U., Graf, R., and Braus, G. H. (1990) *Mol. Gen. Genet.* **224,** 57–64